MADRID
inter.noise 2019
June 16 - 19
NOISE CONTROL FOR A BETTER ENVIRONMENT

Diffracted acoustic field above a wall containing a rectangular parallelepipedic shape

Ben Hamouda Safa[1]
Khanfir Adel [1]
Faiz Adil[2]
Ducourneau Joël[2]
Chevret Patrick[3]
Nasri Rachid[1]

[1]**Laboratoire de Mécanique Appliquée et Ingénierie, Université de Tunis El Manar**
BP 37, Le Belvédère, 1002 Tunis, Tunisie

[2]**Laboratoire d'Énergétique et de Mécanique Théorique et Appliquée**
2 Avenue de la Foret de Haye 54518 Vandœuvre-lès-Nancy, France

[3]**Institut National de Recherche et Sécurité**
1, Rue du Morvan CS 60027, 54519 Vandœuvre-lès-Nancy, France

ABSTRACT

Industrial noise can lead hearing loss for employees working in workshops. These losses can, in the end, be recognized as occupational deafness. In order to better control noise levels in industrial premises, it is necessary to focus on the interaction phenomena between the sound field and the walls of the premises, which may present a regular or irregular relief. In this work, we are interested in walls that contain geometric irregularities and focus in particular on predicting the sound pressure of the field diffused by rectangular parallelepipedic shapes. A theoretical model has been developed for this purpose. It consists in superimposing the different diffracted acoustic fields by the thin rigid rectangular plates that constitute the parallelepipedic shape. To do this, a combination of the image source method and the Kobayashi Potential Theoretical Model (KP) was implemented. The theoretical model was compared with the results of the numerical simulation (Finite Element Method) and the experimental results obtained in the semi-anechoic room of the INRS (French National Research and Safety Institute). Different geometric configurations were studied by changing the sizes and spacing between volumes. For most configurations, the acoustic pressure profile simulated by our model is comparable to the experimental and numerical data on a wide bandwidth (from 200 Hz to 2500 Hz).

benhamoudasafa1@gmail.com
rachid.nasri@enit.rnu.tn

Keywords: Diffraction, sound reflected pressure prediction, relief facings
I-INCE Classification of Subject Number: 23

2. INTRODUCTION

Industrial premises are often delimited by relief walls (furniture, wall with periodic or aperiodic geometry, ...). This type of relief often contains rectangular parallelepiped shapes whose acoustic behaviour has to be studied to know the total sound pressure field in the local. This work consists in modeling the diffracted acoustic field by each rigid facing of rectangular parallelepipedic shapes representative of relief walls in order to determine the total reflected acoustic field. Thus, we combinated the Kobayashi Potential (KP) model [1] to determine the diffracted acoustic field on each rigid facing, and the image source method [2], to take into account the different acoustic fields reflected by the infinite rigid plane. The KP model has been already used to predict the scattering sound field over periodic facing walls containing rectangular cavities [3]. In our case, it is important to clearly distinguish the facets insonified by the source for which the KP model will be applied from those that are in the acoustic shadow region and for which no acoustic field will be taken into account.

First, we will present the development of our theoretical model then, the experimental part that allowed the validation of the model on an elementary rectangular relief. Validation by the use of the Finite Elements Method was also carried out.

2. THEORETICAL STUDY

Let's consider an infinitely rigid large screen containing a rigid parallelepipedic shape which dimensions are $(2a, 2b, 2d)$ along (x, y, z) axis respectively. The cartesian coordinate system (O, x, y, z) is centered in the upper surface f_0. Let Φ_{inc} be the incident plane wave. Φ_d is the field diffracted by the parallelepipedic shape and Φ_r is the specular reflected field by the infinite plane surface given by $z = -2d$ for $|x|>$ a and $|y|>$ b as shown in the figure 1.

The surfaces of the parallelepiped $(f_0, f_1, f_2, f_3, f_4)$ are described by the plane equations written respectively as :

$$\begin{cases} z = 0 \\ x = a \\ y = b \\ x = -a \\ y = -b \end{cases} \quad (1)$$

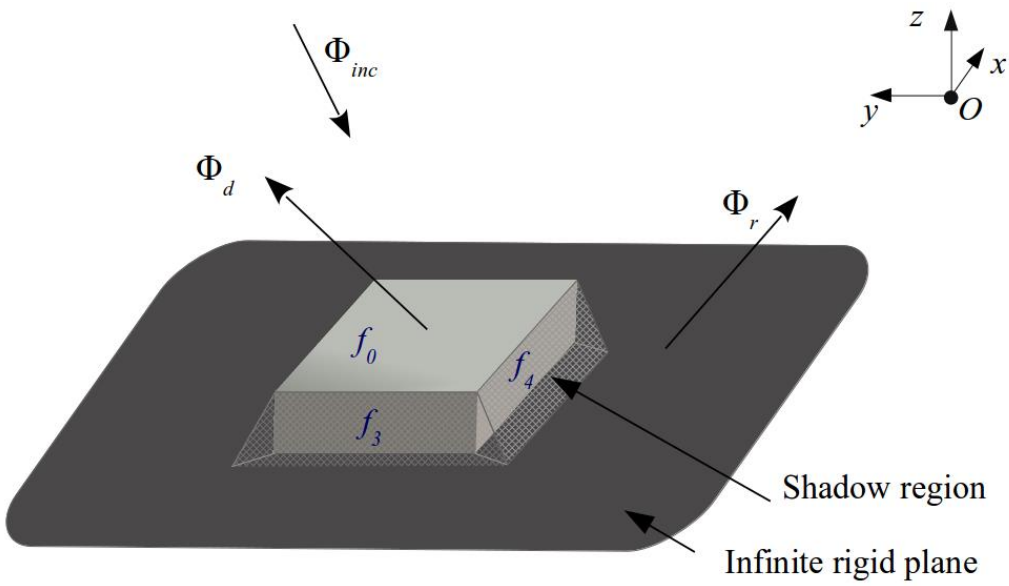

Figure 1: Geometry of the problem

The shape of the relief generates a shadow region around it (figure 1). In the figure, f_3 and f_4 are included in the shadow region. This depends on the position of the source. In this region, the incident and the specularly reflected fields are equal to zero and the diffracted fields depends on which surfaces are insonified. Therefore, a calculation of the shadow region function has been achieved. It is expressed by the following formula:

$$\begin{aligned}\psi(x,y,z) = H[(z-z_s)(x+x_s)-z_s(x-x_s)] \\ \times H[z_s(y-y_s)+(z-z_s)(b-y_s)] \\ \times H[z_s(y-y_s)-(b+y_s)(z-z_s)]\end{aligned} \quad (2)$$

where, H is the heavyside function, x_s , y_s and z_s are the coordinates of the spherical source and

$$\psi(x,y,z) = \begin{cases} 0 \text{ in the shadow region} \\ 1 \text{ in the complementary space} \end{cases}$$

for $\{-2d \le z < 0,\ |x|>a,\ |y|>b\} \cup \{z \ge 0, \forall\ x, y\}$

The total acoustic field Φ^{tot} above the wall includes the incident field Φ_{inc}, the specularly reflected field Φ_r and the diffracted field Φ_d. It is written as follows:

$$\Phi^{tot} = \Phi_{inc} + \Phi_r + \Phi_d \quad (3)$$

where,

$$\Phi_d = \Phi_d^{\text{direct}} + \Phi_d^{image} \quad (4)$$

Φ_d is obtained by superimposing the direct diffracted field Φ_d^{direct} (insonified region) and Φ_d^{image} which includes $\Phi_{d,r}$ ("diffracted then specularly reflected") and $\Phi_{r,d}$ ("specularly

reflected then diffracted").

$$\Phi_d^{direct} = \sum_{i=0}^{2} \Phi_{\mathrm{d}}^{i} \qquad \text{and} \qquad \Phi_d^{\mathrm{image}} = \sum_{i=1}^{2} \Phi_{\mathrm{d,r}}^{i} + \sum_{i=1}^{2} \Phi_{\mathrm{r,d}}^{i} \tag{5}$$

where *i* characterize the insonified surfaces.

$$\Phi_{inc}(x,y,z) = Ae^{jk_1x}e^{jk_2y}e^{jk_3z} \tag{6}$$

$$\Phi_r(x,y,z) = Ae^{jk_1x}e^{jk_2y}e^{-jk_3(z+4d)} \tag{7}$$

A is the amplitude of the incident field.

The velocity potential Φ_d^i of each surface must satisfy two boundary conditions on the planes defined in the equations (1). In the case of f_0 for exemple, the boundary conditions are given by:

$$\frac{\partial}{\partial z}\left(\Phi_{inc} + \Phi_d^0\right) = 0 \quad \text{for} \quad |x| \le a, |y| \le b \text{ and } z = 0 \tag{8}$$

$$\Phi_{inc} \text{ and } \Phi_d^i \text{ are continus for } |x| > a, |y| > b \text{ and } z = 0 \tag{9}$$

Equation (8) means that the total acoustic velocity is equal to zero on the rigid plate. The condition (9) express the continuity of the potential functions outside to the plate in the plane z = 0.

According to the KP method, the diffracted acoustic field is given by:

$$\begin{aligned}\Phi_{\mathrm{d}}^0 = \sum_{\mu=0}^{1}\sum_{\nu=0}^{1}\sum_{m\ge 0}\sum_{n\ge 0}\iint_{\mathbb{R}^2{}_+} \mathcal{A}_{mn}^{0(\mu,\nu)} \mathrm{J}_{2m+1+\mu}(\alpha)\mathrm{J}_{2n+1+\nu}(\beta) \\ \times \cos\left(\alpha\xi - \mu\frac{\pi}{2}\right)\cos\left(\beta\eta - \nu\frac{\pi}{2}\right)\mathrm{e}^{-\sqrt{\left(\frac{\alpha}{a}\right)^2+\left(\frac{\beta}{b}\right)^2-k^2}z}\mathrm{d}\alpha\mathrm{d}\beta\end{aligned} \tag{10}$$

where $\xi = \frac{x}{a}$, $\eta = \frac{y}{b}$, $\vec{k}$ is the wave vector defined as $\vec{k} = k_1\vec{x} + k_2\vec{y} + k_3\vec{z}$, and

$$\mathcal{A}_{mn}^{0,\mu,\nu} = \begin{cases} A_{mn}^0 & \text{if } (\mu,\nu) = (0,0) \\ B_{mn}^0 & \text{if } (\mu,\nu) = (0,1) \\ C_{mn}^0 & \text{if } (\mu,\nu) = (1,0) \\ D_{mn}^0 & \text{if } (\mu,\nu) = (1,1) \end{cases} \tag{11}$$

represent the modal amplitudes.

The functions of ξ and η in the above equation are expanded in terms of Jacobi's polynomials then projected into the functional space of the same polynomials [4]. Then we obtain:

$$\sum_{m,n..0} A_{mn}^{0,\mu,\nu} \iint_{\square_+^2} \frac{J_{2m+1+\mu}(\alpha)J_{2s+1+\mu}(\alpha)}{\alpha^2} \frac{J_{2n+1+\nu}(\beta)J_{2t+1+\nu}(\beta)}{\beta^2} \sqrt{\left(\frac{\alpha}{a}\right)^2 + \left(\frac{\beta}{b}\right)^2 - k^2}\, d\alpha d\beta$$

$$= j^{1+\mu+\nu} k_3 A \frac{J_{2s+1+\mu}(k_1 a)}{k_1 a} \frac{J_{2t+1+\nu}(k_2 b)}{k_2 b} \tag{12}$$

The general solutions for the potential function are given by the linear combination of m and n with the modal amplitudes. Thus, we obtain a system of four matrix equations as shown in (13):

$$\begin{aligned} &[A_{mn}^0][I(2m, 2n, 2s+1, 2t+1)] = [L(2s+1, 2t+1)] \\ &[B_{mn}^0][I(2m, 2n+1, 2s+1, 2t+2)] = [L(2s+1, 2t+2)] \\ &[C_{mn}^0][I(2m+1, 2n, 2s+2, 2t+1)] = [L(2s+2, 2t+1)] \\ &[D_{mn}^0][I(2m+1, 2n+1, 2s+2, 2t+2)] = [L(2s+2, 2t+2)] \end{aligned} \tag{13}$$

where,

$$I(2m+\mu, 2n+\nu, 2s+1+\mu, 2t+1+\nu) = \iint_{\mathbb{R}_+^2} \frac{J_{2m+1+\mu}(\alpha)J_{2u+1+\mu}(\alpha)}{\alpha^2} \frac{J_{2n+1+\nu}(\beta)J_{2s+1+\nu}(\beta)}{\beta^2} \sqrt{\frac{\alpha^2}{a^2} + \frac{\beta^2}{b^2} - k^2}\; d\alpha d\beta \tag{14}$$

and

$$L(2s+1+\mu, 2t+1+\nu) = j^{1+\mu+\nu} k_3 A \frac{J_{2u+1+\mu}(k_1 a)}{k_1 a} \frac{J_{2t+1+\nu}(k_2 b)}{k_2 b} \tag{15}$$

The determination of the diffracted then specularly reflected field $\Phi_{d,r}^0$ is based on the image source method. This field is considered as it is was scattered from the image of f_0 behind the $z = -2d$ plane. In this case, the coordinates of the image source are $(x, y, -z - 4d)$ (see figure 2).

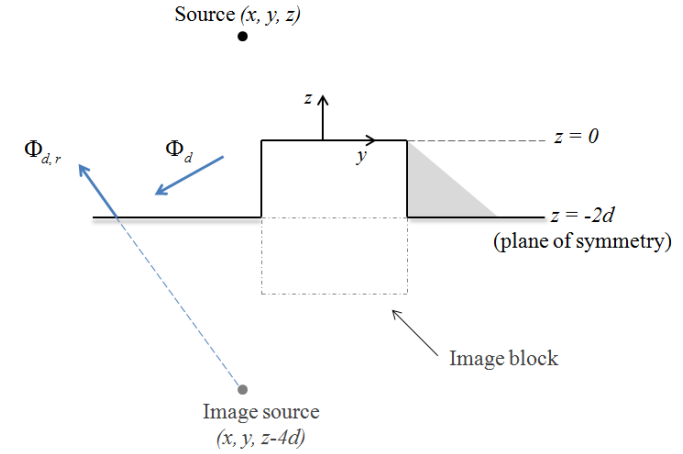

Figure 2: Illustration of the image source method

The problem is solved by applying the same procedure used to calculate Φ_d^0 to the other insonified plates. The double integrals are devided in real and imaginary parts after transforming them into polar coordinates [5]. Then, for $\Phi_{r,d}$ the incident field is supposed

Φ_r (source-mage method) and $\Phi_{d,r}$ is considered like it is diffracted from the imaginary surface symetric to the appropriate real surface.

3 Experimental process

3.1 Description of the experiment

The experiment was achieved in the semi-anechoic chamber of the French National Research and Safety Institute for the Prevention of Occupational Accidents and Deseases (INRS). The parallelepipedic blocks were made of tiled polystyrene in order to model the total reflection of the incident wave.
The experience was achieved using the following equipment:

- Pioneer loudspeaker TSE1077 type and 8cm in diameter,
- B&K 1405 noise generator,
- Fifteen B&K 4935 microphones of 1/4 inch,
- B&K 2694 Deltatron conditioner,
- Power APK 2000 amplifier,
- GQ 1031 Equalizer.

A source was suspended above the wall facing. It was linked to the generator that emits white noise through the equalizer and the amplifier. The measurements were made along a line of 45 microphones spaced by 5.5 cm. For this, we used an antenna of 15 microphones positioned three times along the x axis (figure 3).

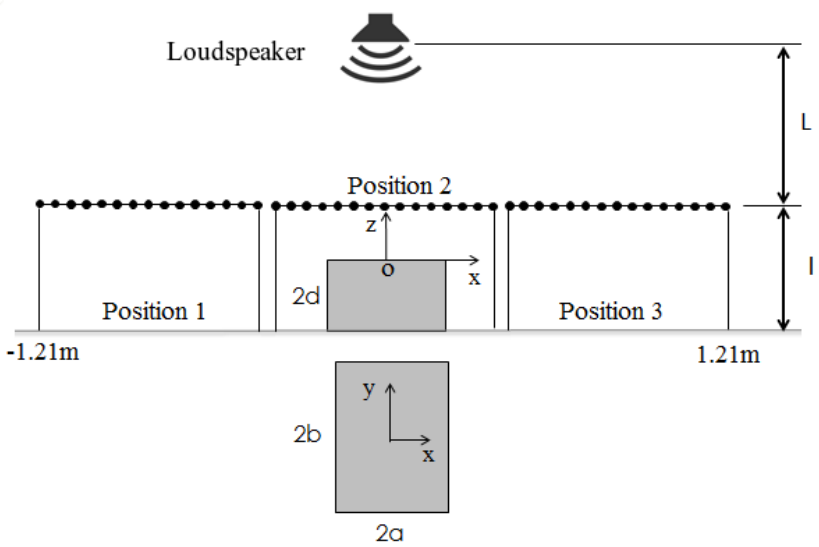

Figure 3: Experimental procedure

In order to have the same source in the experiment and our model we decomposed the spherical wave into a plane wave spectrum [6].
The measured acoustic pressure profiles are normalized with respect to the signal of the

central microphone in order to compare clearly the numerical and the experimental results independently of the real source power.

3.2 FEM Modeling

In this model, we used COMSOL (4.2) for modeling experience. The figure 4 shows a representation of our model. To simulate a perfectly reflecting wall, we used steel. We applied the boundary conditions on the outgoing block and floor to eliminate any structural vibration. To simulate an open field, we applied perfectly Matched Layer PML edges. A source is placed above the study structure. A pressure profile will be obtained above the structure for different frequencies.

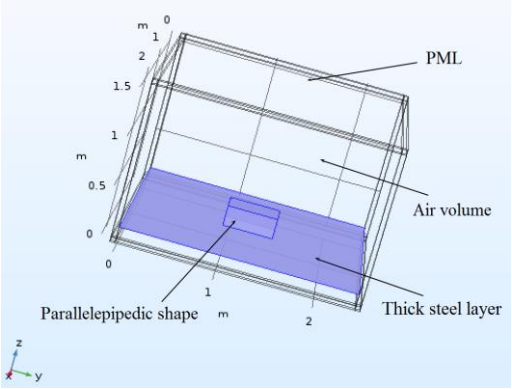

Figure 4 : FEM representation

3.2 Results and comparisons

Figure (5) shows a comparison between the sound pressure amplitudes obtained for the analytical model and the experiment for the frequencies 250, 800, 1400 and 1700 Hz. The results were obtained for an elementary rectangular parallelepiped of $(0.52 \times 0.34 \times 0.2)m^3$ in dimensions. A second validation was carried out for the same relief but by inverting the dimensions along *(Ox)* and *(Oy)* axis $(0.34 \times 0.52 \times 0.2)m^3$. The figure (6) presents the corresponding comparisons for 250, 500, 800 and 1400 Hz, between the results obtained with our model, the experiment and Finite Element Method. In both case, the pressure profiles have been divided by the pressure module obtained at the microphone array center. These profiles correspond to a configuration performed where the source and the sensors are located at 1.45 m and 0.4 m respectively above to the wall $(z = -2d)$.

For this type of elementary relief, a good agreement between the analytical model and the experimental results has been observed for the different frequencies tested. The Finite Element Method shows limitations in high frequencies.

For both configurations, we remark some disagreement between the compared results in the extremities of the pressure profiles. This can probably be explained by the analytical boundary condition in which the rigid plane is supposed infinetly large (no edges). In addition, the source is supposed to be spherical in the decomposition process to plane waves, but it is not perfectly spherical in reality.

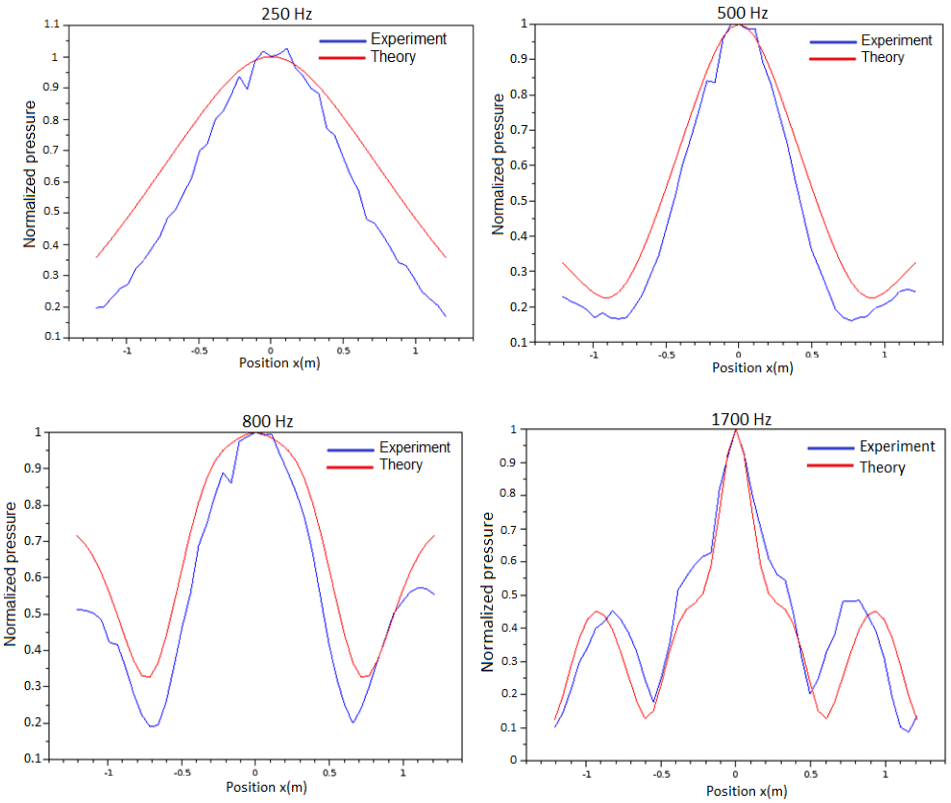

Figure 5: Normalized acoustic pressure at 0.4m above a relief of $(0.52 \times 0.34 \times 0.2)m^3$

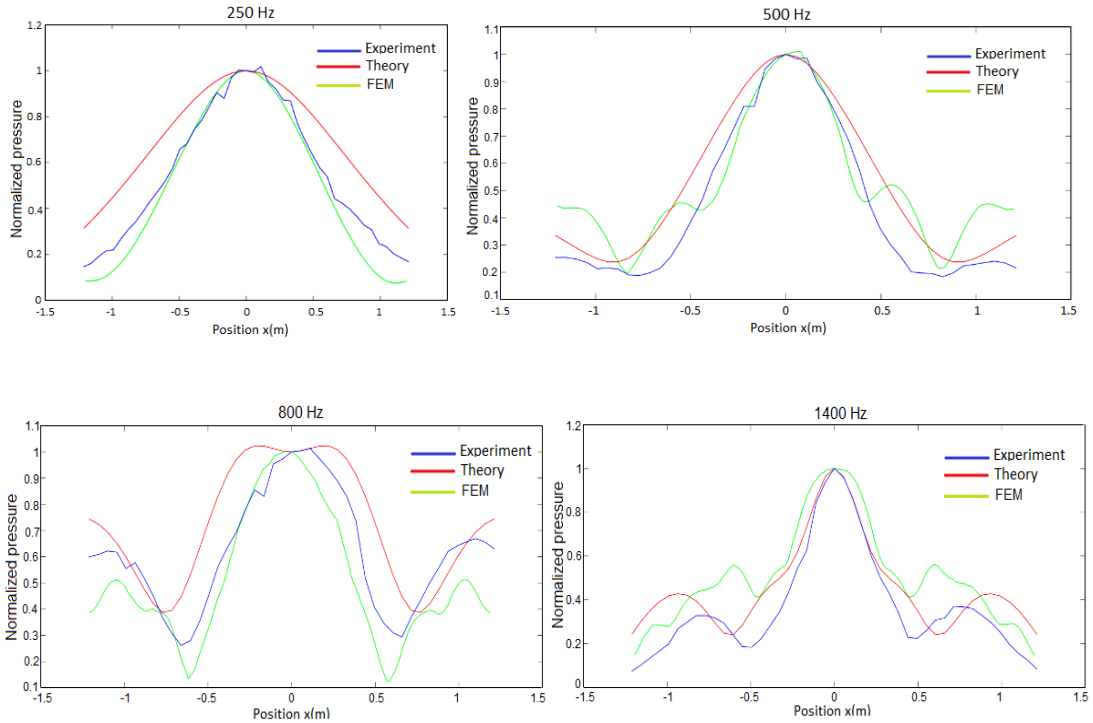

Figure 6: Normalized acoustic pressure at 0.4m above a relief of $(0.34 \times 0.52 \times 0.2)m^3$

4. CONCLUSION

The diffraction of acoustic field by a wall facing containing a parallelepipedic shape was evaluated for different dimensions and frequencies. The KP and image source methods was used as theorical models. For most configurations and despite some low differences observed between the theoretical results and the experimental and numerical data, the model developed is promising.

This study will be generalized to the case of gratings of rectangular parallelepipedic shapes. Parallel and non parallel configurations will be studied. An analysis of the model with and without coupling between the blocks leads to understand the influence of the frequency and the spacings between them.

REFERENCES

1. K. Hongo and H. Sugaya. Diffraction of an acoustic plane wave by a rectangular plate. *Journal of applied physics*, 82(6):2719–2729, 1997.

2. S. M. Dance and B. M. Shield. The complete image-source method for the prediction of sound distribution in non-diffuse enclosed spaces. *Journal of Sound and Vibration*, 201(4) :473 – 489, 1997.

3. A. Khanfir, A. Faiz, J. Ducourneau, and J. Chatillon. Scattering sound field prediction over periodic facing walls containing rectangular cavities. In *Acoustics 2012*, Nantes, 2012.

4. M. Abramowitz, I. A. Stegun, and Others. *Handbook of mathematical functions : with formulas, graphs, and mathematical tables*. 55, 1972.

5. M. Hill and I. Robinson. d2lri : A nonadaptive algorithm for two-dimensional cubature. *Journal of Computational and Applied Mathematics*, 112(1-2):121–145, 1999.

6. A. Khanfir, A. Faiz, J. Ducourneau, J. Chatillon, S. Lami, Scattered acoustic field above a grating of parallel rectangular cavities, *Journal of Sound and Vibration* 332 (4):1047–1060, 2013.